Nuclear Physics A554 (1993) 493–508
North-Holland

NUCLEAR
PHYSICS A

Heavy-ion charge exchange in the eikonal approximation

C.A. Bertulani[1]

National Superconducting Cyclotron Laboratory, Michigan State University, East Lansing, MI 48824-1321, USA

Received 9 July 1992
(Revised 12 November 1992)

Abstract: In high-energy collisions ($E_{lab} > 50$ MeV/nucleon) the eikonal approximation provides a transparent description of heavy-ion exchange reactions. The formalism is applied to the reaction $^{13}N(^{13}C, ^{13}N)^{13}C$ at 70 MeV/nucleon. The relative contributions of pion- and rho-exchange are determined. It is found that heavy-ion reactions are more sensitive to the one-pion exchange component of the interaction than nucleon-induced charge exchange. The cross section for double charge exchange are estimated, which could be useful for future experiments.

1. Introduction

Charge-exchange reactions, i.e. (p, n), (n, p) reactions, are an important tool in nuclear structure physics, providing a measure of the Gamow-Teller strength function in the nuclear excitation spectrum [for a review, see, e.g., ref. [1]]. Experiments with heavy-ion charge-exchange reactions like (^{6}Li, ^{6}He), (^{12}C, ^{12}N) or (^{12}C, ^{12}B) are also becoming common[2,3]), one of the advantages being that both initial and final states involve charged particles, so that a better resolution can often be achieved.

But, apart from this aspect, heavy-ion charge-exchange reactions can help us to understand the underlying nature of the exchange mechanism. On microscopic grounds charge exchange is accomplished through charged meson exchange, mainly π- and ρ-exchange. It is well known that neutron-proton scattering at backward angles results from small angle (low momentum transfer) charge exchange, and is one of the main pieces of evidence for the pion-exchange picture of the nuclear force. The width of the peak is roughly given by the exchanged pion momentum divided by the beam momentum. Therefore, a similar enhancement in the 180° elastic scattering of nuclei should be seen in charge exchange between mirror pairs of nuclei.

Charge exchange between mirror nuclei is particularly interesting because at small angles the exchange has zero momentum transfer. Looking at forward angles also

Correspondence to: Dr. C. Bertulani, National Superconducting Cyclotron Laboratory, Michigan State University, East Lansing, MI 48824-1321, USA.

[1] Permanent address: Instituto de Física, Universidade Federal do Rio de Janeiro, 21945 Rio de Janeiro, Brazil.

has the advantage of eliminating competing processes, namely proton-neutron transfer. Another important advantage of mirror-nuclei charge exchange over (p, n) reactions is that the strong absorption of heavy ions selects large impact parameters and therefore emphasizes the longest range part of the charge-exchange force.

A reasonably good candidate for the investigation of charge exchange between mirror nuclei is the reaction $^{13}C(^{13}N, ^{13}C)^{13}N$ since ^{13}C targets are now available and a relatively intense ^{13}N beam can be produced. This reaction has been performed recently at the Superconducting Cyclotron of Michigan State University and the analysis of the results are under progress [4]). This pair of mirror nuclei is also suitable because the first excited state ($\frac{3}{2}^-$) lies relatively high in energy (3.51 MeV), so that a clear separation can be done between ground-state and excited-state transitions. Also, these nuclei have a single nucleon on the $1p_{1/2}$ orbit. Since the reaction is very peripheral, one expects that the charge-exchange process is practically determined by the participation of these valence nucleons. Therefore, this reaction should be a clear probe of charge exchange in a nuclear environment.

It is the aim of this paper to develop a simple description of charge-exchange reactions at intermediate and high energy in terms of what we believe to be the most important ingredients, namely the microscopic π- and ρ-exchange potentials. An eikonal approach to the nucleus-nucleus scattering is used. This is done in sect. 2. Simple expressions are found which can be useful for estimation purposes in the planning of future experiments. The dependence of the cross sections on the parameters used in this formalism is studied in detail in sect. 3 where an application is done for the reaction $^{13}C(^{13}N, ^{13}C)^{13}N$ at 70 MeV/nucleon. Our conclusions are given in sect. 4.

2. Amplitudes and cross sections

2.1. EIKONAL DESCRIPTION OF CHARGE-EXCHANGE REACTIONS

We will investigate the effect of π- and ρ-exchange in nucleus-nucleus reactions at intermediate energies, and particularly the reaction $^{13}C(^{13}N, ^{13}C)^{13}N$ at 70 MeV/nucleon.

In DWBA the matrix element for this reaction is given by

$$T_{if} = \langle \Psi_{k'}^{(-)}(\boldsymbol{R}) \Phi_f(\boldsymbol{r}) | V(\boldsymbol{R}, \boldsymbol{r}) | \Psi_k^{(+)}(\boldsymbol{R}) \Phi_i(\boldsymbol{r}) \rangle , \tag{1}$$

where $\Psi_{k'}^{(\pm)}(\boldsymbol{R})$ is the distorted wavefunction of the nuclei in the center of mass, having momentum $\boldsymbol{k}$, and $\Phi_{i,f}(\boldsymbol{r})$ are the intrinsic wavefunctions of the nuclei before and after the interaction, respectively. The interaction potential responsible for the charge exchange between the nuclei is given by $V(\boldsymbol{R}, \boldsymbol{r})$, where $\boldsymbol{R}$ is the relative coordinates between the centre of mass of the two nuclei, and $\boldsymbol{r}$ denotes the internal coordinates of the participant nucleons with respect to the c.m. of nuclei (see fig. 1).

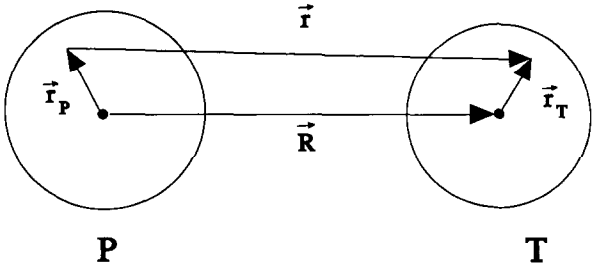

Fig. 1. Coordinates used in the text. R is the distance between the center of mass of the nuclei. r_P and r_T denote the distance of the participant nucleons to the center of the projectile, P, and the target, T, respectively.

Since the reaction occurs at very forward angles, $\theta \ll 1$, and small energy transfer, $\Delta E/E_{\rm lab} \ll 1$, we use the eikonal approximation for the c.m. scattering, i.e.,

$$\Psi_{k'}^{(-)*}(\boldsymbol{R})\Psi_{k}^{(+)}(\boldsymbol{R}) = \exp\{-i\boldsymbol{Q}\cdot\boldsymbol{R} + i\chi(b)\}\,, \tag{2}$$

where $\boldsymbol{Q} = \boldsymbol{k}' - \boldsymbol{k}$, $b = |\boldsymbol{R}\times\hat{\boldsymbol{k}}|$ and

$$\chi(b) = -\frac{i}{\hbar v}\int_{-\infty}^{\infty} U^{\rm opt}(z', b)\,{\rm d}z' + i\phi_{\rm C}(b)\,. \tag{3}$$

$U^{\rm opt}$ is the optical potential for the elastic scattering and $\phi_{\rm C}(b)$ is the Coulomb phase,

$$\phi_{\rm C}(b) = \frac{2Z_1Z_2e^2}{\hbar v}\ln(kb)\,. \tag{4}$$

This phase reproduces the Coulomb scattering amplitude when calculated in the eikonal approximation.

At collisions around 50 MeV/nucleon the phase $\chi(b)$ can be constructed from a fitting to the elastic-scattering data. The optical potential obtained from such a fit can then be used in eq. (3). At higher energies, above 100 MeV/nucleon, the phase $\chi(b)$ will be predominantly imaginary and can be constructed from the t-matrix for nucleon-nucleon scattering [5]).

Eq. (1) can be written as

$$T_{\rm if} = \int {\rm d}^3R\,\langle\Phi_{\rm f}^{\rm P}(\boldsymbol{r}_{\rm P})\Phi_{\rm f}^{\rm T}(\boldsymbol{r}_{\rm T})|\,V(\boldsymbol{r})\exp\{-i\boldsymbol{Q}\cdot\boldsymbol{R} + i\chi(b)\}|\Phi_{\rm i}^{\rm P}(\boldsymbol{r}_{\rm P})\Phi_{\rm i}^{\rm T}(\boldsymbol{r}_{\rm T})\rangle\,, \tag{5}$$

where the indices P and T refer to the intrinsic variables of projectile and target, respectively, and

$$\boldsymbol{r} = \boldsymbol{R} + \boldsymbol{r}_{\rm T} - \boldsymbol{r}_{\rm P}$$

is the relative position of the interacting nucleons. $\boldsymbol{r}_{\rm P}$ ($\boldsymbol{r}_{\rm T}$) is the coordinate of the nucleon with respect to the center of the projectile (target) (see fig. 1).

Using the Fourier transform

$$V(\boldsymbol{r}) = \frac{1}{(2\pi)^3} \int \mathrm{d}^3 q \; V(\boldsymbol{q}) \, \mathrm{e}^{i\boldsymbol{q}\cdot\boldsymbol{r}} , \tag{6}$$

expression (5) becomes

$$T_{\mathrm{if}}(\boldsymbol{m}) = \frac{1}{(2\pi)^3} \int \mathrm{d}^3 q \, \mathrm{d}^3 R \, \exp\{-i\boldsymbol{Q}\cdot\boldsymbol{R} + i\boldsymbol{q}\cdot\boldsymbol{R} + i\chi(b)\} \mathcal{M}(\boldsymbol{m}, \boldsymbol{q}) , \tag{7}$$

where

$$\mathcal{M}(\boldsymbol{m}, \boldsymbol{q}) = \langle \Phi_{\mathrm{f}}^{\mathrm{P}}(\boldsymbol{r}_{\mathrm{P}}) \Phi_{\mathrm{f}}^{\mathrm{T}}(\boldsymbol{r}_{\mathrm{T}}) | \mathrm{e}^{-i\boldsymbol{q}\cdot\boldsymbol{r}_{\mathrm{P}}} \, V(\boldsymbol{q}) \, \mathrm{e}^{i\boldsymbol{q}\cdot\boldsymbol{r}_{\mathrm{T}}} | \Phi_{\mathrm{i}}^{\mathrm{P}}(\boldsymbol{r}_{\mathrm{P}}) \Phi_{\mathrm{i}}^{\mathrm{T}}(\boldsymbol{r}_{\mathrm{T}}) \rangle , \tag{8}$$

and $\boldsymbol{m} = (m_{\mathrm{T}}, m'_{\mathrm{T}}, m_{\mathrm{P}}, m'_{\mathrm{P}})$ is the set of angular-momentum quantum numbers of the projectile and target wavefunction. $\boldsymbol{m}$ is measured along the beam axis and the subindices T and P refer to the target and projectile, respectively.

The z-integral in eq. (7) can be performed immediately, resulting in

$$T_{\mathrm{if}}(\boldsymbol{m}) = \frac{1}{(2\pi)^2} \int \mathrm{d}^2 b \, \mathrm{e}^{-i\boldsymbol{Q}\cdot\boldsymbol{b} + i\chi(b)} \int \mathrm{d}^2 q_{\mathrm{t}} \, \mathrm{e}^{i\boldsymbol{q}_{\mathrm{t}}\cdot\boldsymbol{b}} \mathcal{M}(\boldsymbol{m}, \boldsymbol{q}) , \tag{9}$$

where $\boldsymbol{q}$ is now given by $\boldsymbol{q} = \boldsymbol{q}_{\mathrm{t}} + Q_z \hat{\boldsymbol{z}}$. The indices t and z refer to the direction perpendicular and parallel to the collision axis, respectively.

The azimuthal integrals in eq. (9) can be also easily performed, resulting in

$$T_{\mathrm{if}}(\boldsymbol{m}) = \frac{1}{2\pi} \sum_{\nu=-\infty}^{\infty} \mathrm{e}^{i\nu\phi} \int_0^{\infty} \mathrm{d}b \, b J_{\nu}(Q_{\mathrm{t}} b) \, \mathrm{e}^{i\chi(b)} \times \int_0^{\infty} \mathrm{d}q_{\mathrm{t}} \, q_{\mathrm{t}} J_{\nu}(q_{\mathrm{t}} b) \int_0^{2\pi} \mathrm{d}\phi_q \, \mathrm{e}^{-i\nu\phi_q} \mathcal{M}(\boldsymbol{m}, \boldsymbol{q}) . \tag{10}$$

For small energy transfers, and in intermediate- or high-energy collisions, the momentum transfer $\boldsymbol{Q}$ is predominantly transverse. This simplifies the calculation by allowing to put $\boldsymbol{q} = \boldsymbol{q}_{\mathrm{t}}$ in eq. (10).

The integral (10) is next written as

$$T_{\mathrm{if}}(\boldsymbol{m}) = \frac{1}{2\pi} \sum_{\nu=-\infty}^{\infty} \mathrm{e}^{i\nu\phi} \int_0^{\infty} \mathrm{d}b \, b J_{\nu}(Q_{\mathrm{t}} b) M(\boldsymbol{m}, \nu, b) \, \mathrm{e}^{i\chi(b)} , \tag{11}$$

where

$$M(\boldsymbol{m}, \nu, b) = \int_0^{\infty} \mathrm{d}q_{\mathrm{t}} \, q_{\mathrm{t}} J_{\nu}(q_{\mathrm{t}} b) \int_0^{2\pi} \mathrm{d}\phi_q \, \mathrm{e}^{-i\nu\phi_q} \, \mathcal{M}(\boldsymbol{m}, \boldsymbol{q}) . \tag{12}$$

The differential cross section is obtained by an average of initial spins and sum over final spins ($m_{\mathrm{P(T)}}$; $m'_{\mathrm{P(T)}} = \pm\frac{1}{2}$ for the $1\mathrm{p}_{1/2}$ orbital in $^{13}\mathrm{C}$ and $^{13}\mathrm{N}$),

$$\frac{\mathrm{d}\sigma}{\mathrm{d}\Omega} = \frac{k'}{k} \left(\frac{\mu}{2\pi\hbar^2} \right)^2 \frac{1}{(2j_{\mathrm{P}}+1)(2j_{\mathrm{T}}+1)} \sum_{\boldsymbol{m}} |T_{\mathrm{if}}(\boldsymbol{m})|^2 , \tag{13}$$

where μ is the reduced mass of the projectile+target system. The azimuthal integration can be done immediately, and we can write

$$\frac{\mathrm{d}\sigma}{\mathrm{d}\Omega}=\frac{k'}{k}\left(\frac{\mu}{4\pi^2\hbar^2}\right)^2(2j_\mathrm{P}+1)^{-1}(2j_\mathrm{T}+1)^{-1}$$
$$\times\sum_{\nu,\boldsymbol{m}}\left|\int_0^\infty \mathrm{d}b\, bJ_\nu(Q_\mathrm{t}b)M(\boldsymbol{m},\nu,b)\,\mathrm{e}^{i\chi(b)}\right|^2. \tag{14}$$

Since in high-energy collisions $Q_\mathrm{t}\simeq k\sin\theta$, $\mathrm{d}\Omega\simeq 2\pi Q_\mathrm{t}\,\mathrm{d}Q_\mathrm{t}/k^2$ and, using the integral

$$\int J_\nu(Q_\mathrm{t}b)J_\nu(Q_\mathrm{t}b')Q_\mathrm{t}\,\mathrm{d}Q_\mathrm{t}=\frac{1}{b}\,\delta(b-b'), \tag{15}$$

we can write the total cross section as

$$\sigma=2\pi\int_0^\infty b\mathscr{P}(b)\,\mathrm{d}b, \tag{16}$$

where $\mathscr{P}$ is interpreted as the probability of one-boson exchange at the impact parameter b and is given by

$$\mathscr{P}(b)=\frac{k'}{k}\left(\frac{1}{4\pi^2\hbar v}\right)^2(2j_\mathrm{P}+1)^{-1}(2j_\mathrm{T}+1)^{-1}\exp\{-2\,\mathrm{Im}\,\chi(b)\}\sum_{\nu,\boldsymbol{m}}|M(\boldsymbol{m},\nu,b)|^2, \tag{17}$$

where $\mathrm{Im}\,\chi(b)$ is the imaginary part of the eikonal phase.

Eqs. (14) and (17) are the basic results of the eikonal approach to the description of heavy-ion charge-exchange reactions at intermediate and high energies. They can also be used for the calculation of the excitation of Δ-particles in nucleus–nucleus peripheral collisions. The essential quantity to proceed further is the matrix element given by eq. (8) which is needed to calculate the impact-parameter-dependent amplitude $M(\boldsymbol{m},\nu,b)$ through eq. (12). The magnitude of this amplitude decreases with the decreasing overlap between the nuclei, i.e. with the impact parameter b. At small impact parameters the strong absorption will reduce the charge-exchange probability. Therefore, we expect that the probability given in eq. (17) is peaked at the grazing impact parameter.

2.2 PION- AND RHO-EXCHANGE BETWEEN PROJECTILE AND TARGET NUCLEONS

In momentum representation the pion+rho-exchange potential is given by

$$V(\boldsymbol{q})=-\frac{f_\pi^2}{m_\pi^2}\frac{(\boldsymbol{\sigma}_1\cdot\boldsymbol{q})(\boldsymbol{\sigma}_2\cdot\boldsymbol{q})}{m_\pi^2+\boldsymbol{q}^2}(\boldsymbol{\tau}_1\cdot\boldsymbol{\tau}_2)-\frac{f_\rho^2}{m_\rho^2}\frac{(\boldsymbol{\sigma}_1\times\boldsymbol{q})\cdot(\boldsymbol{\sigma}_2\times\boldsymbol{q})}{m_\rho^2+\boldsymbol{q}^2}(\boldsymbol{\tau}_1\cdot\boldsymbol{\tau}_2), \tag{18}$$

where the pion (rho) coupling constant is $f_\pi^2/4\pi=0.08$ ($f_\rho^2/4\pi=4.85$), $m_\pi c^2=$ 145 MeV and $m_\rho c^2=770$ MeV.

The central part of the potential above has a zero-range component, which is a consequence of the point-like treatment of the meson-nucleon coupling. In reality the interaction extends over a finite region of space, so that the zero-range force must be replaced by an extended source function. This can be done by adding a short-range interaction defined at $\boldsymbol{q}=\mathbf{0}$ in terms of the Landau-Migdal parameters g'_π and g'_ρ. We will use $g'_\pi=\frac{1}{3}$ and $g'_\rho=\frac{2}{3}$, which amounts to remove exactly the zero-range interaction [for details, see, e.g. ref. [1])].

Since the ρ-exchange interaction is of very short range, its central part is appreciably modified by the ω-exchange force. The effect of this repulsive correlation is approximated by multiplying V_ρ^{cent} by a factor $\xi=0.4$ and leaving V_ρ^{tens} unchanged since the tensor force is little affected by ω-exchange [6]).

With these modifications the pion+rho-exchange potential can be written as

$$V(\boldsymbol{q})=V_\pi(\boldsymbol{q})+V_\rho(\boldsymbol{q})=[v(\boldsymbol{q})(\boldsymbol{\sigma}_1\cdot\hat{\boldsymbol{q}})(\boldsymbol{\sigma}_2\cdot\hat{\boldsymbol{q}})+w(\boldsymbol{q})(\boldsymbol{\sigma}_1\cdot\boldsymbol{\sigma}_2)](\boldsymbol{\tau}_1\cdot\boldsymbol{\tau}_2)\,, \tag{19}$$

where

$$v(\boldsymbol{q})=v_\pi^{\text{tens}}(\boldsymbol{q})+v_\rho^{\text{tens}}(\boldsymbol{q})\,, \tag{20}$$

and

$$w(\boldsymbol{q})=w_\pi^{\text{cent}}(\boldsymbol{q})+\xi w_\rho^{\text{cent}}(\boldsymbol{q})+w_\pi^{\text{tens}}(\boldsymbol{q})+w_\rho^{\text{tens}}(\boldsymbol{q})\,, \tag{21}$$

with

$$v_\pi^{\text{tens}}(\boldsymbol{q})=-J_\pi\frac{\boldsymbol{q}^2}{m_\pi^2+\boldsymbol{q}^2}\,,\qquad v_\rho^{\text{tens}}(\boldsymbol{q})=J_\rho\frac{\boldsymbol{q}^2}{m_\rho^2+\boldsymbol{q}^2}\,, \tag{22}$$

$$w_\pi^{\text{cent}}(\boldsymbol{q})=-\tfrac{1}{3}J_\pi\left[\frac{\boldsymbol{q}^2}{m_\pi^2+\boldsymbol{q}^2}-3g'_\pi\right],\qquad w_\rho^{\text{cent}}(\boldsymbol{q})=-\tfrac{2}{3}J_\rho\left[\frac{\boldsymbol{q}^2}{m_\rho^2+\boldsymbol{q}^2}-\tfrac{3}{2}g'_\rho\right], \tag{23}$$

$$w_\pi^{\text{tens}}(\boldsymbol{q})=\tfrac{1}{3}J_\pi\frac{\boldsymbol{q}^2}{m_\pi^2+\boldsymbol{q}^2}\,,\qquad w_\rho^{\text{tens}}(\boldsymbol{q})=-\tfrac{1}{3}J_\rho\frac{\boldsymbol{q}^2}{m_\rho^2+\boldsymbol{q}^2}\,. \tag{24}$$

The values of the coupling constants J_π and J_ρ in nuclear units are given by

$$J_\pi=\frac{f_\pi^2}{m_\pi^2}\equiv f_\pi^2\frac{(\hbar c)^3}{(m_\pi c^2)^2}\simeq 400\ \text{MeV}\cdot\text{fm}^3\,,$$

$$J_\rho=\frac{f_\rho^2}{m_\rho^2}\equiv f_\rho^2\frac{(\hbar c)^3}{(m_\rho c^2)^2}\simeq 790\ \text{MeV}\cdot\text{fm}^3\,. \tag{25}$$

Turning off the terms $w_{\pi,\rho}^{\text{cent}}$, or $v_{\pi,\rho}^{\text{tens}}$ and $w_{\pi,\rho}^{\text{tens}}$, allows us to study the contributions from the central and the tensor interaction, and from π- and ρ-exchange, respectively.

Using eq. (19), single-particle wavefunctions, ϕ_{jlm}, and the representations

$$\boldsymbol{\tau}_{\text{P}}\cdot\boldsymbol{\tau}_{\text{T}}=\tau_{\text{P}}^0\tau_{\text{T}}^0+\tau_{\text{P}}^+\tau_{\text{T}}^-+\tau_{\text{P}}^-\tau_{\text{T}}^+,$$

$$\boldsymbol{\sigma}_{\text{P}}\cdot\boldsymbol{\sigma}_{\text{T}}=\sigma_{\text{P}}^0\sigma_{\text{T}}^0+\sigma_{\text{T}}^+\sigma_{\text{P}}^-+\sigma_{\text{P}}^-\sigma_{\text{T}}^+,$$

we get

$$\mathcal{M}(\boldsymbol{m},\boldsymbol{q}) = w(\boldsymbol{q}) \sum_{\mu\lambda} \langle \phi^{(\pi)}_{jlm'_{\mathrm{T}}} | \sigma_\mu \tau_\lambda \, \mathrm{e}^{i\boldsymbol{q}\cdot\boldsymbol{r}_{\mathrm{T}}} | \phi^{(\nu)}_{jlm_{\mathrm{T}}} \rangle \langle \phi^{(\nu)}_{jlm'_{\mathrm{P}}} | \sigma_\mu \tau_\lambda \, \mathrm{e}^{-i\boldsymbol{q}\cdot\boldsymbol{r}_{\mathrm{P}}} | \phi^{(\pi)}_{jlm_{\mathrm{P}}} \rangle$$

$$+ v(\boldsymbol{q}) \sum_{\mu\mu'\lambda} \hat{q}_\mu \hat{q}'_\mu \langle \phi^{(\pi)}_{jlm'_{\mathrm{T}}} | \sigma_\mu \tau_\lambda \, \mathrm{e}^{i\boldsymbol{q}\cdot\boldsymbol{r}_{\mathrm{T}}} | \phi^{(\nu)}_{jlm_{\mathrm{T}}} \rangle \langle \phi^{(\nu)}_{jlm'_{\mathrm{P}}} | \sigma_\mu \tau_\lambda \, \mathrm{e}^{-i\boldsymbol{q}\cdot\boldsymbol{r}_{\mathrm{P}}} | \phi^{(\pi)}_{jlm_{\mathrm{P}}} \rangle \,, \qquad (26)$$

where

$$\hat{q}_{\mu=0} = q_z/q \,, \qquad \hat{q}_{\mu=+} = \mp \frac{(q_x \pm i q_y)}{\sqrt{2}q} \,, \qquad (27)$$

or, simply

$$\hat{q}_\mu = \sqrt{\tfrac{4}{3}\pi}\, Y_{1\mu}(\hat{\boldsymbol{q}}) \,. \qquad (28)$$

Eq. (26) reduces to

$$\mathcal{M}(\boldsymbol{m},\boldsymbol{q}) = w(\boldsymbol{q}) \sum_{\mu} \langle \phi_{jlm'_{\mathrm{T}}} | \sigma_\mu \, \mathrm{e}^{i\boldsymbol{q}\cdot\boldsymbol{r}} | \phi_{jlm_{\mathrm{T}}} \rangle \langle \phi_{jlm'_{\mathrm{P}}} | \sigma_\mu \, \mathrm{e}^{-i\boldsymbol{q}\cdot\boldsymbol{r}} | \phi_{jlm_{\mathrm{P}}} \rangle$$

$$+ \tfrac{4}{3}\pi v(\boldsymbol{q}) \sum_{\mu\mu'} Y_{1\mu}(\hat{\boldsymbol{q}})\, Y_{1\mu'}(\hat{\boldsymbol{q}}) \langle \phi_{jlm'_{\mathrm{T}}} | \sigma_\mu \, \mathrm{e}^{i\boldsymbol{q}\cdot\boldsymbol{r}} | \phi_{jlm_{\mathrm{T}}} \rangle \langle \phi_{jlm'_{\mathrm{P}}} | \sigma_{\mu'} \, \mathrm{e}^{-i\boldsymbol{q}\cdot\boldsymbol{r}} | \phi_{jlm_{\mathrm{P}}} \rangle \,. \qquad (29)$$

Expanding $\mathrm{e}^{i\boldsymbol{q}\cdot\boldsymbol{r}}$ into multipoles we can write

$$\langle \phi_{jlm'} | \sigma_\mu \, \mathrm{e}^{i\boldsymbol{q}\cdot\boldsymbol{r}} | \phi_{jlm} \rangle = 4\pi \sum_{IM} i^I Y^*_{IM}(\hat{\boldsymbol{q}}) \langle \phi_{jlm'} | j_I(qr)\, Y_{IM}(\hat{\boldsymbol{r}}) \sigma_\mu | \phi_{jlm} \rangle \,. \qquad (30)$$

Since $j_I(qr)\, Y_{IM}(\hat{\boldsymbol{r}})$ is an irreducible tensor,

$$\sigma_\mu j_I(qr)\, Y_{IM}(\hat{\boldsymbol{r}}) = \sum_{I'M'} (I1M\mu | I'M')\, \Psi_{I'M'} \,, \qquad (31)$$

where $\Psi_{I'M'}$ is also an irreducible tensor. Therefore,

$$\langle \phi_{jlm'} | \sigma_\mu j_I(qr)\, Y_{IM}(\hat{\boldsymbol{r}}) | \phi_{jlm} \rangle = \sum_{I'M'} (I1M\mu | I'M') \langle \phi_{jlm'} | \Psi_{I'M'} | \phi_{jlm} \rangle$$

$$= \sum_{I'M'} (I1M\mu | I'M') (jI'mM' | jm') \langle \phi_j || \Psi_{I'} || \phi_j \rangle \,. \qquad (32)$$

Eqs. (29)–(32) allows one to calculate the charge exchange between single-particle orbitals. The quantity needed is the reduced matrix element $\langle \phi_j || [j_I(qr)\sigma \otimes Y_I]_{I'} || \phi_j \rangle$. These are calculated in textbooks of nuclear structure [see, e.g., ref. [7]]. If several orbitals contribute to the process, the respective amplitudes can be added and further on averaged in the cross sections. Before we apply the above formalism to the $^{13}\mathrm{C}(^{13}\mathrm{N}, ^{13}\mathrm{C})^{13}\mathrm{N}$ we shall next discuss the low-momentum-transfer limit of the charge-exchange nucleus–nucleus reaction.

2.2. LOW-MOMENTUM LIMIT AND GAMOW-TELLER MATRIX ELEMENTS

From eqs. (18)-(24) we see that the central interaction $w^{\rm cent}(q)$ dominates the low-momentum scattering $\boldsymbol{q}\sim\boldsymbol{0}$. In this case, the matrix element (26) becomes

$$\mathcal{M}(\mathrm{i}\to\mathrm{f};\ \boldsymbol{q}\sim\boldsymbol{0})\sim C_{\rm spins}w^{\rm cent}(\boldsymbol{q})\mathcal{M}(\mathrm{GT}:\ \mathrm{P}\to\mathrm{P}')\mathcal{M}(\mathrm{GT}:\ \mathrm{T}\to\mathrm{T}')\,, \tag{33}$$

where

$$C_{\rm spins}=\sum_{\mu}\langle I_{\rm P}M_{\rm P}1\mu|I_{\rm P'}M_{\rm P'}\rangle\langle I_{\rm T}M_{\rm T}1\mu|I_{\rm T'}M_{\rm T'}\rangle\,, \tag{34}$$

and $\mathcal{M}(\mathrm{GT}:\ \mathrm{A}\to\mathrm{A}')=\langle\mathrm{A}||\sigma\tau||\mathrm{A}'\rangle$ are the Gamow-Teller (GT) matrix elements for a particular nuclear transition of the projectile (A = P) and of the target (A = T).

Inserting (33) into eq. (12) and using the low-momentum limit, we obtain

$$M(\mathrm{i}\to\mathrm{f};\ b)\sim C_{\rm spins}w^{(0)}\mathcal{M}(\mathrm{GT};\ \mathrm{P}\to\mathrm{P}')\mathcal{M}(\mathrm{GT}:\ \mathrm{T}\to\mathrm{T}')\delta_{\nu 0}\,, \tag{35}$$

where

$$w^{(0)}=2\pi\int_0^{q_{\rm cut}}\mathrm{d}q\,qw^{\rm cent}(\boldsymbol{q})\,, \tag{36}$$

where $q_{\rm cut}$ is a cutoff momentum, up to which value the low-momentum approximation can be justified.

With these approximations, a general expression can be obtained from eq. (14),

$$\frac{\mathrm{d}\sigma}{\mathrm{d}\Omega}(\boldsymbol{q}\sim\boldsymbol{0})=\frac{k'}{k}\left(\frac{\mu}{4\pi^2\hbar^2}\right)^2[w^{(0)}]^2F(\theta)B(\mathrm{GT}:\ \mathrm{P}\to\mathrm{P}')$$
$$\times B(\mathrm{GT}:\ \mathrm{T}\to\mathrm{T}')\sum_{\rm spins}[C_{\rm spins}]^2\,, \tag{37}$$

where

$$B(\mathrm{GT}:\ \mathrm{A}\to\mathrm{A}')=|\langle\mathrm{A}'||\sigma\tau||\mathrm{A}\rangle|^2 \tag{38}$$

is the Gamow-Teller transition density for the nucleus A. The sum over spins includes an average over initial spins and a sum over the final spins of the nuclei.

With these approximations the scattering angular distribution is solely determined by the function

$$F(\theta)=\left|\int\mathrm{d}b\,bJ_0(kb\sin\theta)\,e^{i\chi(b)}\right|^2. \tag{39}$$

In the sharp-cutoff limit ($\exp[i\chi(b)]=\Theta(b-R)$), this function reduces to the very simple result

$$F(\theta)=\frac{R^2}{k^2\sin^2\theta}J_1^2(kR\sin\theta)\,, \tag{40}$$

which displays a characteristic diffraction pattern.

From the above discussion, we see that the ability to extract information on the Gamow-Teller transition densities in a simple way depends on the validity of the

low-momentum-transfer assumption. We shall test this assumption, using the results obtained above, in the special case of the $^{13}C(^{13}N, ^{13}C)^{13}N$ reaction at 70 MeV/nucleon.

3. Application to the reaction $^{13}C(^{13}N, ^{13}C)^{13}N$

3.1. MATRIX ELEMENTS FOR THE VALENCE NUCLEONS

We assume that the pion or rho is exchanged between the neutron in the $1p_{1/2}$ orbital of ^{13}C and the proton of the $1p_{1/2}$ orbital of ^{13}N. Configuration mixing is not included for simplicity.

Using eq. (A.2.24) of ref. [7]) one finds

$$\langle p_{1/2}||[j_I(qr)\sigma\otimes Y_I]_{I'}||p_{1/2}\rangle = -\frac{1}{2\sqrt{3\pi}}\begin{cases}\mathscr{F}_0 & \text{if } I=0,\ I'=1\\ 2\sqrt{2}\mathscr{F}_2 & \text{if } I=2,\ I'=1\\ 0 & \text{otherwise},\end{cases} \tag{41}$$

where

$$\mathscr{F}_I = \int_0^\infty R^2_{1p_{1/2}}(r) j_I(qr) r^2\,dr. \tag{42}$$

The above result means that only transitions with $\Delta l = 0$ and 2 in the $1p_{1/2}$ orbital are allowed. We calculate the radial form factors $\mathscr{F}_0$ and $\mathscr{F}_2$ using harmonic-oscillator functions for the $1p_{1/2}$ orbitals in ^{13}N and ^{13}C:

$$R_{1p_{1/2}}(r) = \left(\frac{8}{3\pi^{1/2}a^5}\right)^{1/2} r\,e^{-r^2/a^2}, \tag{43}$$

where $a = (\hbar/m_N\omega)^{1/2}$ is the oscillator parameter. For ^{13}C and ^{13}N we take $a = 1.55$ fm.

We find

$$\mathscr{F}_0 = (1-\tfrac{1}{6}q^2a^2)\,e^{-q^2a^2/4}, \tag{44}$$

and

$$\mathscr{F}_2 = \tfrac{1}{6}q^2a^2\,e^{-q^2a^2/4}. \tag{45}$$

The matrix element (32) becomes

$$\begin{aligned}&\langle\phi_{jlm'}|\sigma_\mu j_I(qr)\,Y_{IM}(\hat{\boldsymbol{r}})|\phi_{jlm}\rangle\\ &\quad= -\frac{1}{2\sqrt{3\pi}}\mathscr{F}_0(q)(010\mu\,|\,1\mu)(\tfrac{1}{2}1m\mu\,|\,\tfrac{1}{2},\,m+\mu)\,\delta_{I0}\,\delta_{m',m+\mu}\\ &\qquad-\sqrt{\frac{2}{3\pi}}\mathscr{F}_2(q)(21M\mu\,|\,1,\,M+\mu)(\tfrac{1}{2}1m,\,M+\mu\,|\,\tfrac{1}{2},\,m+M+\mu)\,\delta_{I2}\,\delta_{m',m+M+\mu}.\end{aligned} \tag{46}$$

Eq. (30) is then

$$\langle \phi_{jlm'} | \sigma_\mu \, \mathrm{e}^{i\boldsymbol{q}\cdot\boldsymbol{r}} | \phi_{jlm} \rangle = -\frac{1}{\sqrt{3}} (\tfrac{1}{2}1 m, m'-m \,|\, \tfrac{1}{2}m') \times \{ \mathscr{F}_0(q) \, \delta_{m'-m,\mu} - 4\sqrt{\tfrac{2}{3}\pi} (21, m'-m-\mu, \mu \,|\, 1, m'-m) \mathscr{F}_2(q) \} , \tag{47}$$

where we used $(010\mu \,|\, 1\mu) = 1$.

The expression for $\langle \phi_{jlm'} | \sigma_\mu \, \mathrm{e}^{-i\boldsymbol{q}\cdot\boldsymbol{r}} | \phi_{jlm} \rangle$ will be the same as above, since this expression does not change under the substitution $\boldsymbol{q} \to -\boldsymbol{q}$. Therefore, we can write in general form

$$\langle \phi_{jlm'} | \sigma_\mu \, \mathrm{e}^{\pm i\boldsymbol{q}\cdot\boldsymbol{r}} | \phi_{jlm} \rangle = \mathscr{C}_0(m, m', \mu) \mathscr{F}_0(q) + \mathscr{C}_2(m, m', \mu, \hat{\boldsymbol{q}}) \mathscr{F}_2(q) , \tag{48}$$

where

$$\mathscr{C}_0(m, m', \mu) = -\frac{1}{\sqrt{3}} (\tfrac{1}{2}1 m, m'-m \,|\, \tfrac{1}{2}m') \, \delta_{m'-m,\mu} , \tag{49}$$

$$\mathscr{C}_2(m, m', \mu, \hat{\boldsymbol{q}}) = 4\sqrt{\tfrac{2}{3}\pi} (\tfrac{1}{2}1 m, m'-m \,|\, \tfrac{1}{2}m') \times (21, m'-m-\mu, \mu \,|\, 1, m'-m) \, Y^*_{2,m'-m-\mu}(\hat{\boldsymbol{q}}) . \tag{50}$$

Inserting these results in eq. (29), we find

$$\begin{aligned} \mathscr{M}(\boldsymbol{m}, \boldsymbol{q}) = w(\boldsymbol{q}) \sum_\mu & [\mathscr{C}_0(m_\mathrm{T}, m'_\mathrm{T}, \mu) \mathscr{F}_0(q) + \mathscr{C}_2(m_\mathrm{T}, m'_\mathrm{T}, \mu, \hat{\boldsymbol{q}}) \mathscr{F}_2(q)] \\ & \times [\mathscr{C}_0(m_\mathrm{P}, m'_\mathrm{P}, \mu) \mathscr{F}_0(q) + \mathscr{C}_2(m_\mathrm{P}, m'_\mathrm{P}, \mu, \hat{\boldsymbol{q}}) \mathscr{F}_2(q)] \\ & + \tfrac{4}{3}\pi v(\boldsymbol{q}) \sum_{\mu\mu'} Y_{1\mu}(\hat{\boldsymbol{q}}) Y_{1\mu'}(\hat{\boldsymbol{q}}) \\ & \times [\mathscr{C}_0(m_\mathrm{T}, m'_\mathrm{T}, \mu) \mathscr{F}_0(q) + \mathscr{C}_2(m_\mathrm{T}, m'_\mathrm{T}, \mu, \hat{\boldsymbol{q}}) \mathscr{F}_2(q)] \\ & \times [\mathscr{C}_0(m_\mathrm{P}, m'_\mathrm{P}, \mu') \mathscr{F}_0(q) + \mathscr{C}_2(m_\mathrm{P}, m'_\mathrm{P}, \mu', \hat{\boldsymbol{q}}) \mathscr{F}_2(q)] . \end{aligned} \tag{51}$$

Finally, the integral (12) is easily performed, and we show it in the appendix.

3.2. NUMERICAL RESULTS

Since there are no data available on the elastic scattering of the reaction $^{13}\mathrm{C} + ^{13}\mathrm{N}$ at 70 MeV/nucleon, we use an optical potential which fits the reaction $^{12}\mathrm{C} + ^{12}\mathrm{C}$ at 85 MeV/nucleon. We use the eikonal approximation for elastic scattering,

$$f(\theta) = ik \int J_0(kb)[1 - \mathrm{e}^{i\chi(b)}] b \, \mathrm{d}b , \tag{52}$$

with the phase given by eq. (3). In fig. 2 we show the result of such calculation, using $U^{\mathrm{opt}}(r) = V(r) + iW(r)$ with Woods-Saxon form for the real and imaginary potentials. The parameters chosen were

$$\begin{aligned} V_0 &= -80 \text{ MeV} , \qquad R_V = 3.76 \text{ fm} , \qquad a_V = 0.74 \text{ fm} , \\ W_0 &= -41 \text{ MeV} , \qquad R_W = 4.2 \text{ fm} , \qquad a_W = 0.73 \text{ fm} . \end{aligned} \tag{53}$$

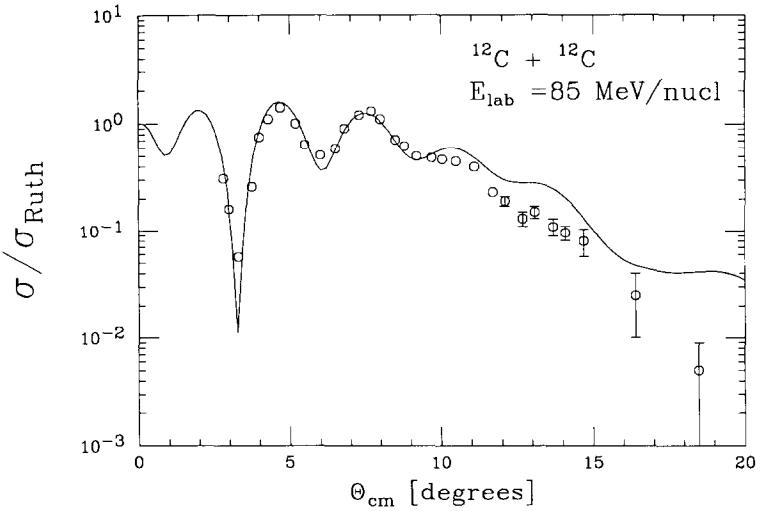

Fig. 2. Ratio between the elastic and the Rutherford cross section for the reaction $^{12}C+^{12}C$ at 85 MeV/nucleon. The data are from ref. [8]). The curve is a theoretical calculation based on the eikonal approximation (see text for details).

We see that the agreement with the experimental data [from ref. [8])] is good, especially at small scattering angles. Since the charge-exchange reaction is very forward peaked, the bad fit at large angles ($\theta > 10°$) will not be relevant for our calculations, and we will use this eikonal wavefunction in the charge-exchange calculation.

Fig. 3 shows the contributions from π- (dashed curve) and from ρ-exchange (dotted curve) to the charge-exchange probability as a function of the impact parameter. The solid curve is the total probability. The exchange probability is peaked at grazing impact parameters: at low impact parameters the strong absorption makes the probability small, whereas at large impact parameters it is small because of the short-range of the exchange potentials. The value of the exchange probability at the peak is about 1.2×10^{-5}. It is clear from fig. 3 that the process is dominated by π-exchange. At small impact parameters the short-range ρ-exchange contribution is large due to a larger overlap between the nuclei.

In fig. 4 the differential cross section is plotted. One observes that at very forward angles the π-exchange contributes to the largest part of the cross section. But ρ-exchange is important at large angles. It has the net effect of smoothing out the dips of the angular distribution. Since π-exchange is of longer range than ρ-exchange, the dips caused by the two contributions are displaced; the ones from ρ-exchange alone are located at larger angles, as expected from the relation $\theta \sim 1/r$. If we put $\mathcal{F}_{0,2} = 1$ and $\exp[i\chi(b)] = 1$, we obtain that at very small scattering angles the π- and ρ-exchange contributions to the differential cross sections are approximately of the same magnitude. This means that ρ-exchange is more important when distortions are weaker, i.e., in nucleon-nucleon or nucleon-nucleus scattering [1]).

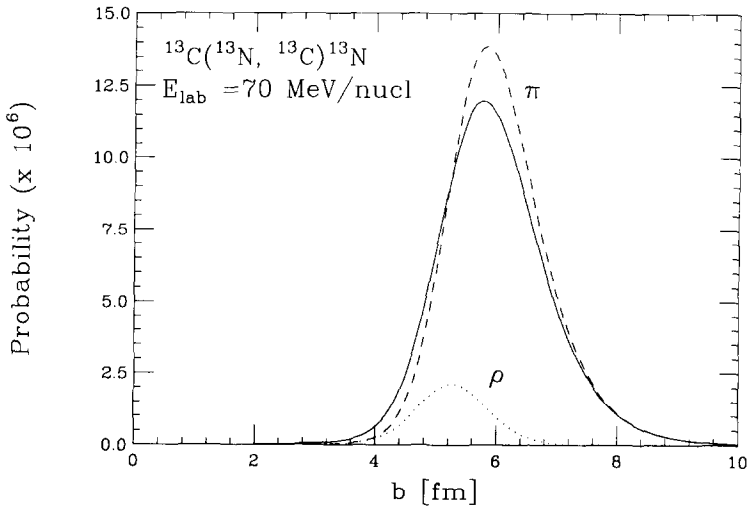

Fig. 3. Probability for π- (dashed curve) and ρ-exchange (dotted curve) in the reaction $^{13}C(^{13}N, ^{13}C)^{13}N$ at 70 MeV/nucleon, as a function of the impact parameter. The solid curve represents the result of the full interaction.

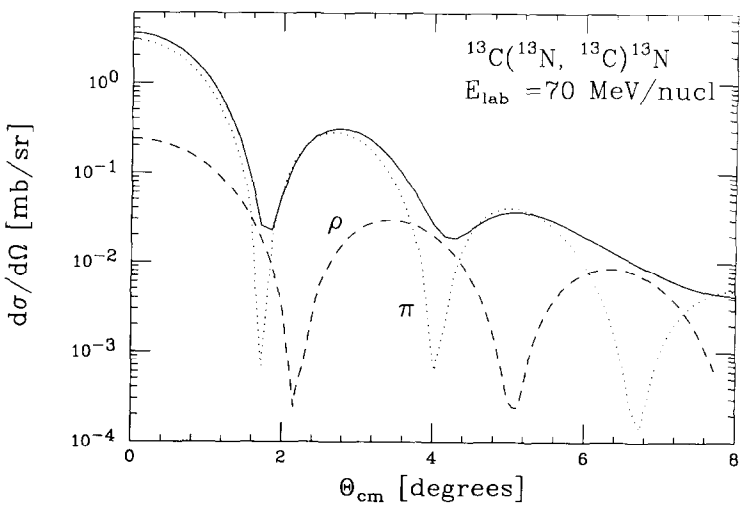

Fig. 4. Angular distribution for charge exchange in the reaction $^{13}C(^{13}N, ^{13}C)^{13}N$ at 70 MeV/nucleon. The contribution from π- (dotted curve) and ρ-exchange (dashed curve) are displayed separately. The solid curve represents the result of the full interaction.

In fig. 5 we show the contributions from the central (dashed) and the tensorial (dotted) part of the total exchange potential ($\pi+\rho$). The probability is dominated by the central interaction. Due to the selection rules which are implicit in the sum over Clebsch-Gordan coefficients, the matrices $M(\boldsymbol{m}, \nu, b)$ are zero if only one of the spins (actually, j_z) is flipped. That is, transitions like ($m_P=+\frac{1}{2}$, $m_T=-\frac{1}{2}$, $m'_P=+\frac{1}{2}$, $m'_T=+\frac{1}{2}$) are absent. The percentage contribution of the other transitions to the total cross section is shown in table 1.

The non-spin-flip components are strongly suppressed and the cross section is dominated by simultaneous spin-flip components, with $\Delta j=0$ (33%) and 2 (16.8%). This can be understood in terms of the contributions of the tensor and the central part of the pion+rho interaction to the heavy-ion charge exchange, as seen in fig. 5. The central (tensor) force is responsible for the $\Delta j=0$ (2) transitions.

In fig. 6 we show the result of using the approximate expression (37) (dashed line). This curve has been obtained by calculating eq. (37) and normalizing the result to match the total differential cross section at 0°. One sees that the agreement with the more elaborate calculation (solid curve) is good at forward angles ($\theta<2°$). At larger angles it fails badly. This result implies that the extraction of Gamow-Teller matrix elements from heavy-ion charge-exchange reactions is possible, as soon as one can have good resolution in the forward-scattering region.

The total cross section obtained is 7.6 μb. The peak value of the differential cross section at 0° is 3.5 mb/sr. These values are of the order of magnitude of the charge-exchange cross sections measured for other systems [3]).

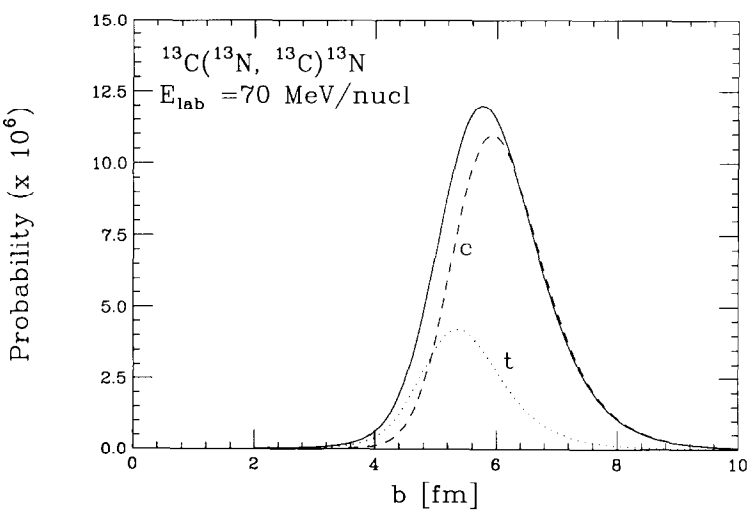

Fig. 5. Probability for charge exchange in the reaction $^{13}C(^{13}N, ^{13}C)^{13}N$ at 70 MeV/nucleon, as a function of the impact parameter. The dashed (dotted) curve represent the contribution of the central (tensor) part of the interaction. The solid curve represents the result of the full interaction.

TABLE 1

Contribution to the total cross section of a particular set of angular-momentum projections

m_P	m'_P	m_T	m'_T	
−	−	−	−	0.1%
−	−	+	+	0.1%
+	+	−	−	0.1%
+	+	+	+	0.1%
−	+	−	+	16.8%
+	−	+	−	16.8%
−	+	+	−	33%
+	−	−	+	33%

Finally, we make a remark on the double exchange reactions. From the values obtained above one sees that the charge-exchange probability as a function of impact parameter is small, of order of 10^{-5}. Even for enhanced transitions, one should not expect an increase higher than a factor 10 in the probability. An estimate of double-charge exchange is obtained from eq. (16), replacing $\mathcal{P}(b)$ by $\frac{1}{2}\mathcal{P}^2(b)$. That is, the ratio between the single- and the double-charge exchange is of order of 10^{-4}–10^{-5}. If the single-step total cross section is of order of tens of microbarns, the double-step one is of order of nanobarns, in the best cases. Similarly, if the peak of the differential cross section at zero degrees is of order of tens of millibarns,

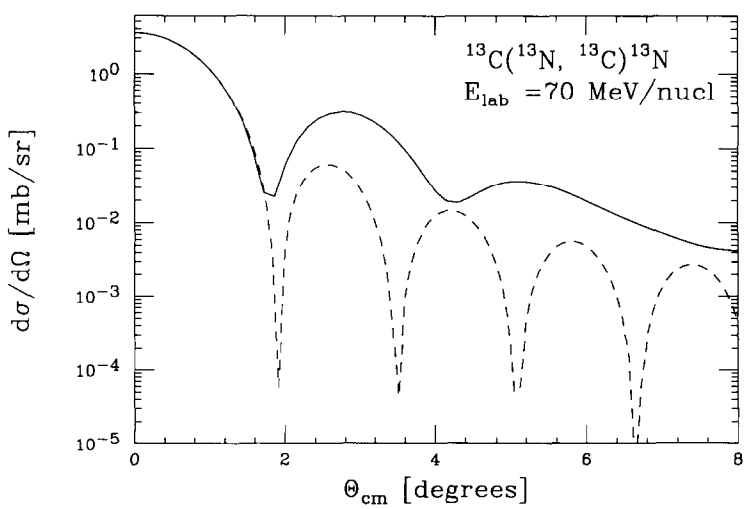

Fig. 6. Angular distribution for charge exchange in the reaction $^{13}C(^{13}N, ^{13}C)^{13}N$ at 70 MeV/nucleon. The solid curve represents the result of the full interaction. Also shown is the result of the approximation (37) (dashed curve).

the corresponding one for double-charge exchange will be of order of microbarns, in the best cases. The measurement of double-charge exchange in heavy-ion collisions will therefore require intense beams and good detection efficiency.

4. Conclusions

It was shown that the eikonal approximation provides a convenient description of heavy-ion charge-exchange reactions at intermediate and high energies. Very useful and transparent expressions can be obtained in this way.

These results have been applied to the reaction $^{13}C(^{13}N, ^{13}C)^{13}N$ at 70 MeV/nucleon. The exchange probability is shown to be very peaked at the grazing impact parameter. This results in typical diffraction patterns in the angular distributions. It was also shown that pion-exchange dominates the process and that the characteristics of the angular distributions are understood in terms of the different ranges of the π- and ρ-exchange mechanism. This is manifest in the smoothing of the angular distributions. The order of magnitude of the differential cross section at 0° and of the total cross section are in reasonably good agreement with the experimental results [3]), giving support to the microscopic picture of π- and ρ-exchange.

The connection of the heavy-ion charge-exchange cross sections to the nuclear Gamow-Teller matrix elements is straightforward in the eikonal formalism. At very forward angles it has been shown that the extraction of Gamow-Teller matrix elements is possible.

The author has benefited from many suggestions and fruitful discussions with G. Bertsch, Brad Sherrill and M. Steiner. This work was partially supported by the National Science Foundation/US under grant 90-17077 and by the CNPq/Brazil.

Appendix

CALCULATION OF $M(m, \nu, b)$

Using

$$Y_{lm}(\hat{\boldsymbol{q}}_t) = (-1)^{(l+m)/2}\left(\frac{2l+1}{4\pi}\right)^{1/2}\frac{[(l-m)!(l+m)!]^{1/2}}{(l-m)!!(l+m)!!}e^{im\phi}, \quad \text{if } l+m=\text{even},$$

$$= 0, \qquad \text{otherwise}, \tag{A.1}$$

and

$$\int_0^{2\pi} e^{i(m-\nu)\phi}\,d\phi = 2\pi\delta_{m,\nu} \tag{A.2}$$

and the definitions (12) and (51), we find

$$M(\boldsymbol{m}, \nu, b) = \int_0^\infty \mathrm{d}q\, qJ_\nu(qb)\{w(q)[X_{00}\mathscr{F}_0^2(q) + X_{02}\mathscr{F}_0(q)\mathscr{F}_2(q) + X_{22}\mathscr{F}_2^2(q)]$$
$$+ \tfrac{4}{3}\pi v(q)[W_{00}\mathscr{F}_0^2(q) + W_{02}\mathscr{F}_0(q)\mathscr{F}_2(q) + W_{22}\mathscr{F}_2^2(q)]\}\,, \tag{A.3}$$

$$X_{00} = \delta_{\nu,0} 2\pi \sum_\mu \mathscr{C}_0(m_\mathrm{T}, m'_\mathrm{T}, \mu)\mathscr{C}_0(m_\mathrm{P}, m'_\mathrm{P}, \mu)\,, \tag{A.4}$$

$$X_{02} = 2\pi \sum_\mu \{\mathscr{C}_0(m_\mathrm{T}, m'_\mathrm{T}, \mu)\mathscr{C}_2(m_\mathrm{P}, m'_\mathrm{P}, \mu, \theta = \tfrac{1}{2}\pi, \phi = 0)\, \delta_{\nu,\mu - m'_\mathrm{P} + m_\mathrm{P}}$$
$$+ (m_\mathrm{P}, m'_\mathrm{P}) \leftrightarrow (m_\mathrm{T}, m'_\mathrm{T})\}\,, \tag{A.5}$$

$$X_{22} = 2\pi \sum_\mu \mathscr{C}_2(m_\mathrm{T}\, m'_\mathrm{T}, \mu, \theta = \tfrac{1}{2}\pi, \phi = 0)$$
$$\times \mathscr{C}_2(m_\mathrm{P}, m'_\mathrm{P}, \mu, \theta = \tfrac{1}{2}\pi, \phi = 0)\, \delta_{\nu,2\mu - m'_\mathrm{T} + m_\mathrm{T} - m'_\mathrm{P} + m_\mathrm{P}}\,, \tag{A.6}$$

and

$$W_{00} = 2\pi \sum_{\mu\mu'} \mathscr{C}_0(m_\mathrm{T}, m'_\mathrm{T}, \mu)\mathscr{C}_0(m_\mathrm{P}, m'_\mathrm{P}, \mu')\, Y_{1\mu}(\theta = \tfrac{1}{2}\pi, 0)\, Y_{1\mu'}(\theta = \tfrac{1}{2}\pi, 0)\, \delta_{\nu,\mu+\mu'}, \tag{A.7}$$

$$W_{02} = 2\pi \sum_{\mu\mu'} Y_{1\mu}(\theta = \tfrac{1}{2}\pi, 0)\, Y_{1\mu'}(\theta = \tfrac{1}{2}\pi, 0)$$
$$\times \{\mathscr{C}_0(m_\mathrm{T}, m'_\mathrm{T}, \mu)\mathscr{C}_2(m_\mathrm{P}, m'_\mathrm{P}, \mu', \theta = \tfrac{1}{2}\pi, \phi = 0)\, \delta_{\nu,2\mu' + \mu - m'_\mathrm{P} + m_\mathrm{P}}$$
$$+ (\mu, m_\mathrm{P}, m'_\mathrm{P}) \leftrightarrow (\mu', m_\mathrm{T}, m'_\mathrm{T})\}\,, \tag{A.8}$$

$$W_{22} = 2\pi \sum_{\mu\mu'} Y_{1\mu}(\theta = \tfrac{1}{2}\pi, 0)\, Y_{1\mu'}(\theta = \tfrac{1}{2}\pi, 0)\mathscr{C}_2(m_\mathrm{T}, m'_\mathrm{T}, \mu, \theta = \tfrac{1}{2}\pi, \phi = 0)$$
$$\times \mathscr{C}_2(m_\mathrm{P}, m'_\mathrm{P}, \mu', \theta = \tfrac{1}{2}\pi, \phi = 0)\, \delta_{\nu,2\mu + 2\mu' + m_\mathrm{T} + m_\mathrm{P} - m'_\mathrm{T} - m'_\mathrm{P}}\,. \tag{A.9}$$

The momentum integral in eq. (A.3) is performed numerically.

References

1) G.F. Bertsch and H. Esbensen, Rep. Prog. Phys. **50** (1987) 607
2) J.S. Winfield, N. Anantaraman, S.M. Austin, L.H. Harwood, J. van der Plicht, H.-L. Wu and A.F. Zeller, Phys. Rev. **C33** (1986) 1333; **C35** (1987) 1166(E)
3) N. Anantaraman, J.S. Winfield, S.M. Austin, J.A. Carr, C. Djalali, A. Gilibert, W. Mittig, J.A. Nolen Jr. and Z.W. Long, Phys. Rev. **C44** (1991) 398
4) B.M. Sherrill, private communication
5) M.S. Hussein, R. Rego and C.A. Bertulani, Phys. Reports **201** (1991) 279
6) M.R. Anastasio and G.E. Brown, Nucl. Phys. **A285** (1977) 516
7) R.D. Lawson, Theory of the nuclear shell model (Clarendon, Oxford, 1980)
8) M. Buenerd, P. Martin, R. Bertholet, C. Guet, M. Maurel, J. Mougey, H. Nifenecker, J. Pinston, P. Perrin, F. Schlusser, J. Julien, J.P. Bondorf, L. Carlen, H.A. Gustafsson, B. Jakobsson, T. Johansson, P. Kristiansson, O.B. Nielsen, A. Oskarsson, I. Otterlund, H. Ryde, B. Schroeder and G. Tibeli, Phys. Rev. **C26** (1982) 1299